Raman Microscopy Investigation of GLP-1 Peptide Association with Supported Phospholipid Bilayers

David A. Bryce,[a] Jay P. Kitt,[a,b] and Joel M. Harris[a,*]

[a]Department of Chemistry, University of Utah, 315 South 1400 East, Salt Lake City, UT 84112

[b]Department of Biomedical Informatics, University of Utah, 421 Wakara Way Ste. 140, Salt Lake City, UT 84108 USA

ABSTRACT

A wide range of important biological processes occur at phospholipid membranes including cell signaling, where a peptide or small molecule targets a membrane-localized receptor protein. In this work, we report the adaptation of confocal-Raman microscopy to quantify populations of *unlabeled* glucagon-like peptide-1 (GLP-1), a membrane-active 30-residue incretin peptide, in supported phospholipid bilayers deposited on the interior surfaces of wide-pore porous silica particles. Quantification of lipid bilayer-associated peptide is achieved by measuring the Raman scattering intensity of the peptide relative to that of the supported-lipid bilayer, which serves as an internal standard. The dependence of the bilayer-associated GLP-1 population on the solution-concentration of GLP-1 produces an isotherm used to determine the equilibrium constant for peptide-bilayer association and the maximum peptide surface coverage. The maximum coverage of GLP-1 in the lipid bilayer was found to be only 1/5th of a full monolayer based on its hydrodynamic radius. The saturation coverage, therefore, is *not limited by the size of GLP-1* but by the ability of the bilayer to accommodate the peptide at high concentrations within the bilayer. Raman spectra show that GLP-1 association with the supported bilayer is accompanied by structural changes consistent with the intercalation of the peptide into bilayer, where the observed increase in acyl-chain order would increase the lipid density and provide free volume needed to accommodate the peptide. These results were compared with previous measurements of the association of fluorescently-labeled GLP-1 with a planar-supported bilayer; the unlabeled peptide exhibits a 3-fold greater affinity for the lipid-bilayer on the porous-silica support suggesting that the fluorescent label alters GLP-1 lipid-bilayer association.

*Corresponding author: harrisj@chem.utah.edu

INTRODUCTION

Molecular interactions at phospholipid bilayers play a critical role in a multitude of biologically-relevant processes. One such role is the interaction of signaling peptides with cell membranes that precedes binding of the peptide to a membrane-localized receptor. Several mechanisms have been proposed for these peptide-bilayer interactions that facilitate the signaling response.[1-3] One premise is that peptide-membrane interactions cause structural organization of the signaling peptide, effectively 'pre-folding' the peptide into a conformation that is favorable for receptor binding. In addition, if the peptide has high affinity for the membrane, the local concentration of signaling peptide in the bilayer can be much greater than in free-solution, increasing the frequency of encounters with membrane-localized receptors. Finally, membrane affiliation limits diffusion of the peptide to a two-dimensional surface, thereby increasing the receptor encounter frequency.

A signaling peptide that has been the subject of numerous investigations is glucagon like peptide-1 (GLP-1), a 30-amino-acid peptide hormone or incretin. GLP-1 is produced by cleavage of the protein proglucagon to a 37-amino-acid peptide, followed by truncation and amidation of the C-terminus, forming a biologically-active incretin peptide.[4] Incretins are known to impact blood-glucose levels; thus, considerable interest has developed for the use of incretins or chemically similar synthetic peptide sequences in treatment of diabetes.[5-7] Several studies have been conducted to assess the membrane activity of GLP-1 including quantifying membrane-associated populations, investigating membrane-binding kinetics, and determining the free-solution and membrane-bound structure of GLP-1.[8-12] Early vibrational spectroscopy (FT-IR and FT-Raman) experiments were carried out to investigate the impact of changes in secondary structure on GLP-1 solubility in aqueous solutions.[8] These studies revealed that variations in solubility correlated with infrared and Raman spectral features consistent with changes in secondary peptide structure. NMR studies have revealed that while GLP-1 in free-solution exists as a random coil, while in micellar membrane models, GLP-1 exhibits two α-helical regions connected by a flexible linkage that allows the hydrophobic and hydrophilic faces of the two helices to align and interact with the amphiphilic interface of a model phospholipid membrane.[9,10]

Single-molecule fluorescence experiments carried out on planar supported phospholipid bilayers have been used to count membrane-localized GLP-1 populations and measure their association and dissociation kinetics.[11,12] These experiments provided insight into peptide-lipid membrane interactions and were used to estimate free-energy barriers for GLP-1 association with the bilayer. GLP-1 residence times at the lipid-bilayer interface indicated the presence of weakly- and strongly-bound GLP-1 populations, consistent with a sequential binding model, where weakly bound molecules can fold into a more strongly-bound state. Because of its 10-fold longer residence time, the strongly-bound form dominates the interfacial population at equilibrium.[12]

While these studies have provided considerable information about membrane-associated GLP-1 populations, several limitations are apparent. In the case of the vibrational spectroscopy study,[8] experiments were carried out on aqueous samples of GLP-1 with or without organic modifiers or on solid pellets of precipitated peptides. While these studies provide insight into structure-solubility relationships for the peptide, they fail to address the interactions of the peptide with lipid membranes. The NMR experiments[9,10] offer insight into structural changes in the peptide that occur upon GLP-1 interaction with a micellar model of a lipid interface but do not produce quantitative information on the population of micelle-associated peptides. Additionally, the micelles used in these experiments are not an ideal model of phospholipid bilayer, and the results do not report lipid organizational changes that may occur upon GLP-1 binding. The single-molecule-fluorescence microscopy experiments were carried out at planar-supported lipid bilayers and addressed peptide quantification, reporting membrane-associated GLP-1 populations, association equilibria, and kinetics. These experiments, however, do not convey information about changes in structure of the lipid membrane upon peptide affiliation. Furthermore, fluorescence microscopy methods also require a fluorescent label be attached to the peptide, possibly influencing the peptide secondary structure and its interactions with the lipid bilayer.

Raman spectroscopy is an attractive method for measuring peptide-lipid bilayer interactions because it is fully compatible with aqueous solutions and provides quantitative and structural information for both proteins[13,14] and phospholipids.[15,16] Phospholipid and peptide detection by Raman scattering from a phospholipid bilayer deposited on a planar support is

challenging, however, due to small Raman scattering cross sections and limited population of molecules that can be probed on a planar surface. Recently, we have reported the preparation of supported phospholipid bilayers deposited on the internal surfaces of large-pore chromatographic silica particles.[17] The high specific surface area within the silica support provides phospholipid concentrations within the particle as high as 0.5M, overcoming the sensitivity challenge of detecting phospholipid bilayers on planar supports. When combined with the excitation and collection efficiency of confocal-Raman microscopy, this approach has allowed measurement of Raman scattering from supported-lipid bilayers on silica surfaces and the binding of proteins to lipid bilayer-immobilized ligands.[18]

In this work, we apply confocal-Raman microscopy to probe *in situ* the interactions between unlabeled GLP-1 and phospholipid bilayers deposited in wide-pore silica. Raman spectra are collected from within-particle supported-lipid bilayers after equilibration with solution-phase GLP-1, allowing *quantitative measurement of the membrane-associated peptide* and investigation of the structural changes in the phospholipid that accompany association of the peptide with the supported bilayer. Membrane-bound GLP-1 populations are quantified using the Raman scattering intensity from the phospholipid as an internal standard.[19,20] Concentration-dependent GLP-1 populations are fit to Langmuir isotherms to determine membrane-association equilibrium constants of unlabeled GLP-1, which are then compared with labeled-GLP-1 results from single-molecule imaging experiments on planar supported bilayers. The isotherms are also used to resolve the concentration-dependent Raman scattering data into component spectra that reveal changes in lipid organization upon association of the peptide with the supported bilayer.

EXPERIMENTAL SECTION

Reagents and materials Spherical, bare chromatographic silica particles were obtained from YMC America (YMC Sil, Allentown, PA); the particles had an average diameter of 10-μm and pore diameter of 29-nm as specified by the manufacturer. Water used in all experiments was filtered using a Barnstead GenPure UV water purification system (ThermoFisher Scientific, Waltham, MA) and had a minimum resistivity of 18.0MΩ·cm. 1-palmitoyl-2-oleoyl-*sn*-glycero-3-phosphocholine (POPC), 1,2-dimyristoyl-*sn*-glycero-3-phosphocholine (DMPC), and 1,2-dipalmitoyl-*sn*-glycero-3-phosphocholine (DPPC) were purchased from Avanti Polar Lipids, Inc. (Alabaster, AL), diluted into chloroform, and stored at -15°C until use. Glucagon-like peptide 1 (GLP-1) in the biologically-active form GLP-1 7-36-NH_2 was purchased from ProSpec Bio (Rehovot, Israel). The peptide was stored as lypholized powder at -18 °C until just before use, at which point it was rehydrated in a dilute aqueous solution of acetic acid. Chloroform (Chromasolv Plus, >99.9%), d,l-phenylalanine (ReagentPlus, >99%), sodium phosphate, sodium chloride (NaCl), calcium chloride ($CaCl_2$), tris(hydroxymethyl)aminomethane (Tris), potassium chloride (KCl), sodium hydroxide, acetic acid, and hydrochloric acid were purchased from Sigma-Aldrich (St. Louis, MO) and used without further purification.

Preparation of within-particle supported phospholipid bilayers. The deposition and characterization of supported bilayers on the pore surfaces of chromatographic silica supports has been described in detail elsewhere.[17] In short, supported bilayers were prepared by vesicle fusion as follows. The spherical 10-μm diameter porous silica particles were first cleaned in base-piranha solution (60/40 concentrated ammonium hydroxide/30% hydrogen peroxide; warning: base-piranha solutions are highly corrosive and strong oxidizers that can react explosively with organics) for ~5 minutes, rinsed in deionized water, and dried at 140 °C overnight. Lipid vesicle dispersions were prepared by hydrating a film of phospholipid, deposited from chloroform solution onto a glass vial surface, with Tris-buffered saline (TBS) buffer (10-mM Tris, 137-mM NaCl, 2.7-mM KCl) containing 5-mM $CaCl_2$ to a final lipid concentration of 2mg/mL. The dispersion was sonicated in a bath sonicator at a temperature above the phospholipid melting transition to form small (~20nm diameter) unilamellar vesicles. Vesicle suspensions were mixed with the cleaned

spherical silica to produce a 1-mg/mL dispersion of particles. This dispersion was sonicated for ~20 min and then stirred with the phospholipid for ~12 hours at a temperature above the lipid melting transition to allow vesicle fusion and bilayer formation to take place. Particles were separated from excess lipid by centrifugation, rinsed in deionized water multiple times with centrifugation, and stored in deionized water at ~5 ºC until use.

Confocal Raman microscopy. The confocal Raman microscope used in this work has been described in detail previously.[21,22] The confocal aperture of the described microscope system is defined in the horizontal dimension by the entrance slit of the monochromator (50 μm) and in the vertical dimension by limiting signal acquisition to 3 pixel rows on the CCD chip (78 μm).[23] The 100× 1.4 NA objective (CFL PLAN APO, Nikon Inc.) produces a confocal probe volume with a waist diameter of ~600 nm[21] and an axial depth of 1.7 μm[24] which is localized entirely within the 10-μm porous silica particles used in this work.

Samples for Raman microscopy were measured in glass well-cells constructed by adhering a ~12-mm length of 10-mm i.d., 13-mm o.d. Pyrex glass tubing to a No. 1 glass coverslip using Devcon 5-min epoxy (ITW Devcon, Danvers, MA). Raman spectra were collected from the interior of individual chromatographic particles as follows: the focused laser beam was translated to the solution-coverslip interface where reflected light from the laser spot was visible in the microscope eyepiece. This reflection of the focused spot was then translated in x,y dimensions to below the center of a particle of interest. The objective was then translated in the *z* dimension until the perimeter of the particle was brought into sharp focus, and the confocal probe volume is centered in the particle. Spectra were acquired for 1-min intervals, truncated to spectral regions of interest, and baseline-corrected by subtraction of a polynomial function fit to peak-free regions of the spectrum. All experiments were carried out at 21°C. When necessary, spectra were normalized to the phospholipid-ester carbonyl stretch. Component spectra were resolved from GLP-1 concentration-dependent data by multidimensional least squares;[25-27] all spectral data analysis was carried out with custom routines written for Matlab (Mathworks, Natick, MA).

RESULTS AND DISCUSSION

Detecting Raman scattering from GLP-1 in phospholipid bilayers. To test the feasibility of detecting GLP-1 associating with supported-lipid bilayers in porous silica using confocal-Raman microscopy, a DPMC bilayer was deposited by vesicle fusion in 29-nm pore diameter silica, as described above. A small aliquot of DMPC-treated particles was mixed for 2 hours in a solution of 10-μM GLP-1 in 50-mM phosphate buffer, transferred to a cell on the microscope stage, and Raman spectra were collected from five particles and averaged. Spectra of control samples were also collected from supported-lipid bilayer particles exposed to 50-mM phosphate buffer containing no GLP-1 and from bare-silica particles (no phospholipid) equilibrated with the 10-μM GLP-1 in phosphate buffer, as above. Raman spectra were baseline-corrected and area-normalized, and are plotted in Figure 1. In spectra of samples with supported-bilayers, Raman bands are observed corresponding to the DMPC phospholipid head-group totally-symmetric C-N stretch (715 cm^{-1}), as well as carbon-carbon and carbon-hydrogen modes from the lipid acyl chains. These include the acyl-chain C-C stretching modes (~1050 – 1130 cm^{-1}), CH_2 twisting mode (1295 cm^{-1}), CH_3 antisymmetric bending mode (1440 cm^{-1}) and CH_2 scissoring mode (shoulder at 1455 cm^{-1}).[16,28] In the case of the supported-lipid bilayer exposed to GLP-1, several peptide Raman peaks appear including the phenylalanine ring-breathing mode (1004 cm^{-1}), and the peptide backbone amide-I mode (1670 cm^{-1}), highlighted in Figure 1.[13,29] Detecting GLP-1 scattering from within the particle is clear evidence of accumulation of the

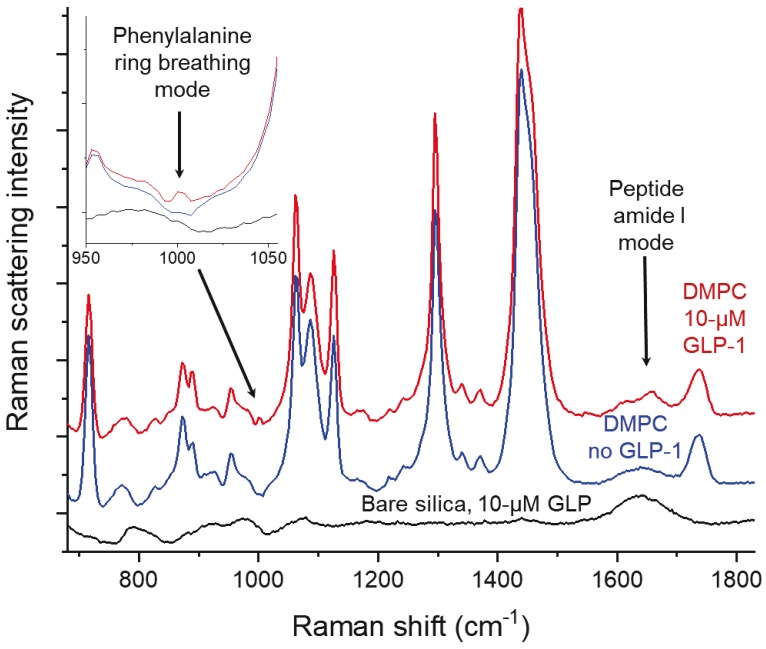

Figure 1. Raman spectra collected from DMPC supported bilayers before (blue) and after (red) exposure to 10-μM GLP-1 solution, and bare silica support particles exposed to the same GLP-1 solution. The peptide phenylalanine ring breathing mode and amide I mode (highlighted) appear in the after exposure DMPC spectrum but are absent in the blank and bare silica spectra. Lipid vibrational modes are described in the text and highlighted in the next figure.

peptide in the supported bilayer, since the 10-μM GLP-1 source-phase concentration is two-orders-of-magnitude below the limit of detecting the peptide in free solution. The results also indicate that accumulation of GLP-1 in the supported-lipid bilayer is selective, where no measurable GLP-1 is observed in the bare silica particle exposed to the 10-μM GLP-1 solution (Figure 1). These observations are consistent with the concept that membrane-association of signaling peptides increases their local concentration relative to free solution, which can increase the frequency of peptide-receptor encounters.[1-3]

The reversibility of the peptide-lipid bilayer interaction was also assessed. Raman spectra from DMPC supported bilayer particles before exposure to 10-μM GLP-1 solution, upon exposure and equilibration, and then after a wash-off where the GLP-1-equilibrated particles are washed with excess (GLP-1 free) phosphate buffer are compared in Supporting Information (Figure S1). In these results, we observe the appearance of peptide Raman bands upon exposure to GLP-1 solution as above. When the GLP-1-exposed sample is then equilibrated with excess buffer containing no GLP-1, Raman bands from the peptide disappear and no evidence of residual GLP-1 can be observed (see Figure S1-B). The exposure to GLP-1 followed by wash-off results in no detectable loss of scattering from the lipid-bands (Figure S1-A) relative to the particle-to-particle variation in band intensities (Figure S1-C); these results indicate that GLP-1 accumulation is not accompanied by displacement of lipid from the bilayer.

Quantifying lipid bilayer-associated GLP-1 and its adsorption isotherm. In order to quantify the GLP-1 population in the lipid bilayer, Raman scattering intensities from the known lipid-bilayer density on the silica surface of the porous-particle can be employed as an internal standard. In this case, quantification of membrane-associated GLP-1 populations is achieved by comparing the scattering intensity of the peptide phenylalanine ring breathing mode to that of the phospholipid head-group C-N stretching mode. We have previously characterized the surface coverage and head-group spacing of supported phospholipid bilayers of DMPC deposited on the pore surfaces of chromatographic silica particles based on carbon analysis, volume-displacement measurements, and the specific surface area of the porous silica support.[17] The total lipid surface coverage (4.8±0.1 μmol/m^2) corresponds to a head-group area of 69 ±1 Å^2 per phospholipid in the

bilayer, which is slightly (~18%) greater than the head-group area of a fluid-phase DMPC vesicle bilayer measured by small-angle neutron scattering experiments.[30] This known phospholipid surface coverage can be used as an internal standard, so that the peptide phenylalanine Raman scattering relative to that of the lipid C-N stretch allows quantification of bilayer-associated GLP-1. Relative Raman scattering responses for phenylalanine and head-group C-N stretch are determined from measurements of standard solutions of DMPC and phenylalanine in a 50:50 isopropyl alcohol:water, spectra of which are presented in Supporting Information (Figure S2). These relative scattering intensities were used to determine a response factor, F, which allows the measured ratio of spectral intensities of phenylalanine ring-breathing mode to C-N head-group stretch and the known surface-density of lipid to predict the surface population of GLP-1 associated with the lipid bilayer:

$$\theta_{GLP-1} = F * \frac{1}{3} * \frac{I_{phen}}{I_{CN}} * \theta_{lipid} \qquad (1)$$

where θ_{GLP-1} and θ_{lipid} are the surface coverages of GLP-1 and lipid (in mol/m^2) respectively, where the factor 1/3rd accounts for the number of phenylalanine residues in GLP-1, and where I_{phen} and I_{CN} are the measured intensities of phenylalanine ring breathing mode and C-N head-group stretch in the calibration sample.

Using this calibration, the surface GLP-1 coverage on silica-supported DMPC bilayers was measured for GLP-1 solution concentrations ranging from 0- to 50-μM. Raman spectra were collected from the center of five supported-bilayer particles at each concentration, baseline

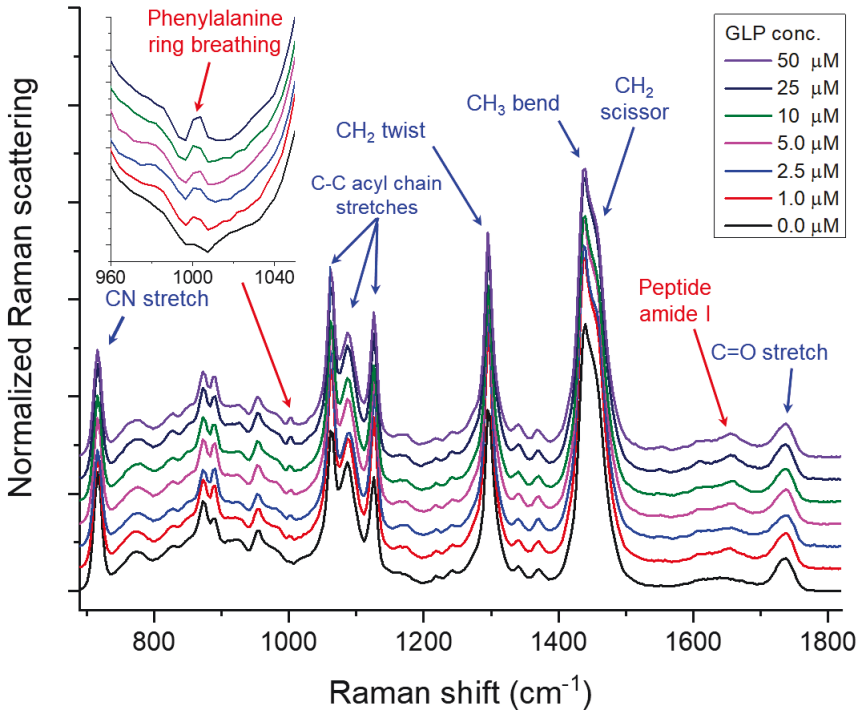

Figure 2. Raman spectra of DMPC supported bilayer particles equilibrated with GLP-1 concentrations from 0 to 50 μM. Selected peptide and lipid Raman scattering modes are noted in red and blue respectively. Concentration-dependent phenylalanine ring breathing intensities are highlighted in the inset.

corrected, and normalized to the area of the phospholipid-ester carbonyl stretch (1737 cm^{-1}). Averaged spectra from each of these experiments are presented in Figure 2, with key phospholipid and peptide Raman bands highlighted. Peptide Raman modes increase and eventually reach a maximum as the solution GLP-1 concentration increases. The relative scattering intensities of the phenylalanine ring-breathing mode of GLP-1 and the lipid C-N head-group stretch were used to quantify the bilayer-associated peptide, and the peptide surface coverages are plotted as a function of solution GLP-1 concentration in Figure 3. The concentration-dependent surface coverage data are well fit by a Langmuir isotherm:

$$\Gamma = \Gamma_{\max} * \frac{K_L[GLP1]}{1+K_L[GLP1]} \qquad (2)$$

where Γ and Γ_{max} in mol/m^2 are the concentration-dependent and maximum GLP-1 coverages, respectively, and K_L is the Langmuir adsorption constant in M^{-1}. The maximum surface coverage determined from these results is Γ_{max} = 6.4±0.4 x10^{-8} mol/m^2, *which is only 21% of the surface density of a full monolayer of GLP-1* based on its hydrodynamic radius.[31,32] This result indicates that the maximum coverage of GLP-1 present in the lipid bilayer is *not limited by the size of GLP-1* but by the ability of the bilayer to accommodate the peptide at high interfacial concentrations.

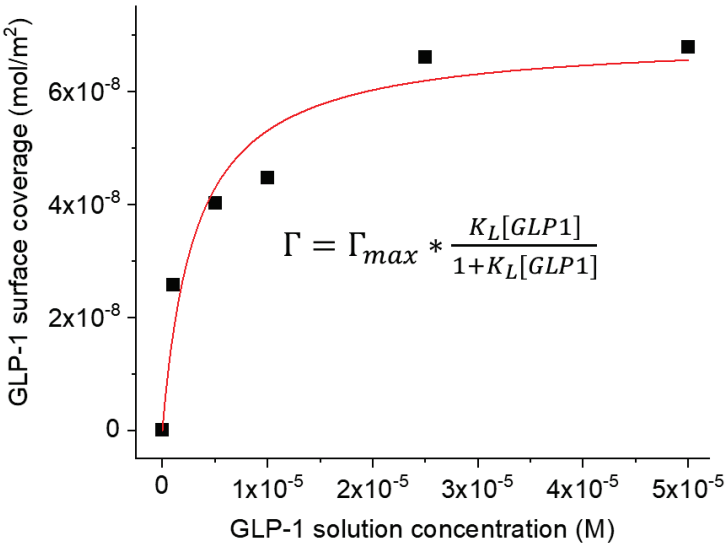

Figure 3. Concentration-dependent GLP-1 surface coverage determined from Raman scattering intensity of the peptide phenylalanine ring-breathing mode and relative to the phospholipid CN head group stretch, fit to Langmuir isotherm (red line). The average uncertainty in GLP-1 surface coverage is 1.1 × 10^{-8} mol/m^2.

Bilayer structural changes in response to GLP-1 accumulation. To investigate the structural changes characteristic of GLP-1 accumulation, it is helpful to resolve the spectral contributions that change with GLP-1 association. Multidimensional-least-squares analysis is used to resolve GLP-1-concentration-dependent Raman scattering data into two spectral components, a fixed or constant component and a GLP-1 concentration-dependent component.[33] Collected data

are expressed as an r x c matrix, $\boldsymbol{D}$, of spectra measured at r wavenumbers arranged in columns corresponding to c different peptide-solution concentrations that drive accumulation of peptide along with changes in the membrane structure. If the shapes of these two component spectra are independent of their relative contributions (*i.e.* only their total amplitudes change), then the data matrix can be represented by the product[25-27] of an r x n matrix of component spectra ($\boldsymbol{A}$) and an n x c matrix ($\boldsymbol{C}$) of component contributions over the c different concentration conditions:

$$D = AC \tag{3}$$

We model the composition matrix ($\boldsymbol{C}$) with $n = 2$ vectors, one of which is a constant (concentration-independent) to capture the Raman scattering from the lipid bilayer that does not change with GLP-1 concentration, while a second tracks the GLP-1 concentration in the bilayer, modeled by a Langmuir isotherm (Equation 2) from the fit of the phenylalanine intensity in Figure 3.

To resolve the spectral components that correspond to constant and Langmuir-response vectors in $\boldsymbol{C}$, the data matrix ($\boldsymbol{D}$) is multiplied by the right-pseudo-inverse of the concentration matrix ($\boldsymbol{C}$) to solve for the least-squares best-fit component spectra ($\hat{\boldsymbol{A}}$):

$$\hat{A} = D\,C^T[CC^T]^{-1} \tag{4}$$

The resulting component spectra are area normalized and presented in Figure 4. The constant or fixed component shows no significant difference from the initial spectrum collected from the DMPC supported bilayer before equilibration with GLP-1. The Langmuir-isotherm component

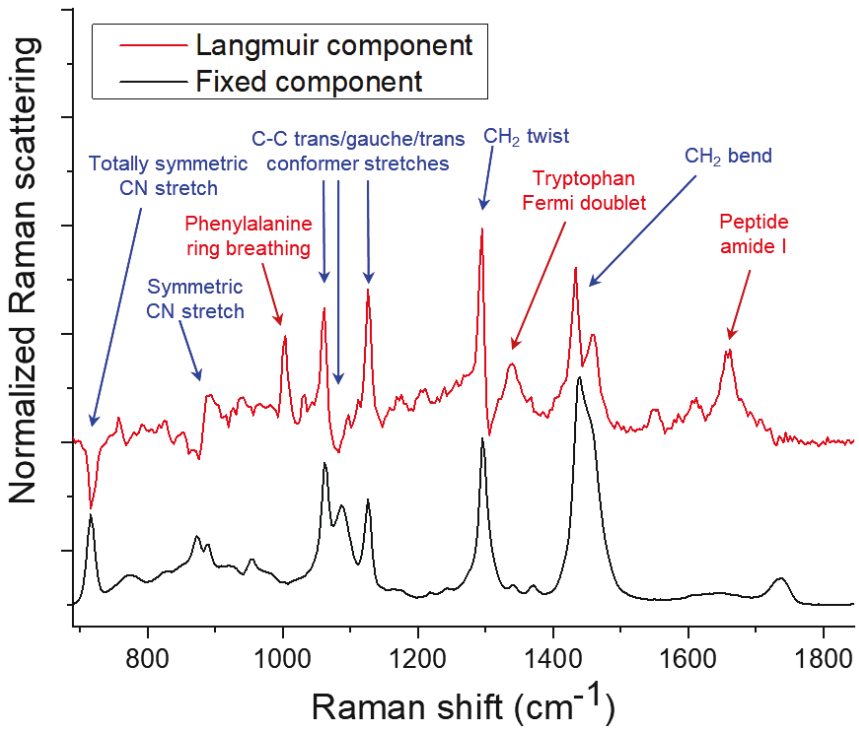

Figure 4. Component spectra produced from linear-least squares analysis of Raman spectra collected from DMPC supported-bilayers exposed to variable concentrations GLP-1 solution, fit to a fixed component (black) and Langmuir isotherm component (red). Spectral features of accumulated protein accumulation (red labels), as well as changes indicative of increased lipid bilayer order (blue labels) appear in the Langmuir component; the fixed component is indistinguishable from spectra collected from a DMPC supported bilayer.

shows several noteworthy spectral features. Prominent scattering appears from the phenylalanine ring-breathing (1004 cm^{-1}), tryptophan Fermi-doublet (~1340 cm^{-1}), and peptide backbone amide I (~1660 cm^{-1}) modes, indicative of peptide accumulation in the supported DMPC bilayer.

More interesting are *several phospholipid Raman bands* present in the Langmuir-isotherm component that are indicative of changes in the lipid membrane structure in response to accumulation of GLP-1. In the acyl-chain carbon-carbon stretching region, sharp increases in the C-C trans-conformers (~1060 and 1125 cm^{-1}) and a corresponding loss of intensity in C-C gauche conformer mode (~1080 cm^{-1}) are observed.[16,34,35] The increase in intensity around 1295 cm^{-1} with corresponding negative-going character at 1305 cm^{-1} is consistent with a decrease in frequency width of the phospholipid CH_2 twisting mode.[36,37] Finally, intensity increases in the CH_2 bending modes (1460 cm^{-1}) can be attributed to correlation-field-induced splitting of the CH_2 bending mode.[16,37,38] All of these GLP-1 dependent changes in the lipid bilayer spectra are consistent with *an increase in acyl-chain order* in the hydrocarbon region of the bilayer[16,39-41] as GLP-1 accumulates in the membrane. This result is surprising in light of previous vibrational spectroscopy investigations of helical peptide incorporation into the bilayer membranes of lipid vesicles, where peptide accumulation results in disordering of the lipid bilayer acyl chains and lowering of the gel to liquid-crystalline phase transition temperature.[42-45] This behavior is similarly observed for small-molecule partitioning into phospholipid vesicle bilayers leading to both disruption of acyl-chain order and lowering of the melting-transition temperature.[46,47]

Ordering of the acyl chains upon accumulation of GLP-1 in the present case may be due to the supported-lipid bilayer needing to create free-volume to accommodate the peptide, while being unable to expand laterally to provide that volume. In phospholipid vesicles, the *membrane area can expand* to provide room for a peptide solute. This increase in membrane area would need to be accompanied by an increase in the internal solution volume within the vesicle. Fortunately, the efficient transport of water through phospholipid membranes can quickly relax any pressure differential caused by the greater membrane area. Based on the permeability coefficient of water through a phospholipid membrane, $k_p = 4.4 \times 10^5$ s^{-1},[48] the flux of water through the membrane of a 5-μm vesicle can exchange its *entire internal volume* in 0.3 msec,[49] faster than is needed to

respond to a change in vesicle membrane area due to a seconds-long accumulation with GLP-1.[12] The resulting expanded membrane is thus disordered by incorporation of the peptide or small molecule solute.

For a lipid bilayer on a solid support however, lateral expansion of a fully-formed lipid bilayer is physically inhibited. In the case of planar-supported lipid bilayers, expansion is limited by barriers on the substrate that confine its area,[50] or in the case of a porous-particle support by the total surface area of the particle.[17] The free volume needed to accommodate the peptide could arise by desorption of phospholipid from the bilayer; however, the solubility of long-chain phospholipids such as DPPC is 'essentially zero' being undetectable at the sub-ppm level.[51] Therefore, desorption of lipid into solution is inhibited by lack of solubility and is thus not a feasible route to creating free volume in bilayer to accommodate a peptide. This conclusion is validated by the results in Figure S1-A, discussed above, where the lipid bilayer signal before accumulation and after GLP-1 saturation and wash-off shows no detectable change in lipid surface coverage. Creation of free volume in a supported lipid bilayer could be generated by the conversion of disordered acyl-chain gauche conformers into ordered all-trans conformers, which is accompanied by an increase in the local density of the lipid bilayer[52,53] providing space for the partitioned peptide. This mechanism provides a physical understanding of the maximum GLP-1 coverage discussed above being limited to a small fraction (21%) of a full monolayer: the incorporation of the peptide into the lipid bilayer requires conversion of lipid acyl chains from gauche- to trans-conformers and is limited by the local change in lipid density that can be achieved through chain ordering.

The results clearly indicate that the GLP-1 affiliation with the bilayer is *not simple adsorption* to the bilayer surface, but rather partitioning *into* the lipid bilayer structure. GLP-1 occupies space in the hydrocarbon core of the bilayer created by forming higher-density and more ordered acyl chains. This structure is consistent with NMR evidence that the hydrophobic and hydrophilic faces of the GLP-1 α-helices align so that the peptide can reside in an amphiphilic region where it interacts with both the head-groups and acyl chains of the lipid bilayer.[9,10] In this region, GLP-1 association could also perturb the head-group structure, which is indeed observed.

Changes in Raman scattering from phospholipid head-group modes correlate with GLP-1 association, including a small decrease in the totally-symmetric CN-head-group stretch (715 cm^{-1}) and a shifting in the symmetric CN-head-group stretching frequency (885 cm^{-1}). The symmetric CN stretch has been shown to be sensitive to phospholipid head-group choline conformation,[54] where in the present case, the shifting of the frequency indicates an increase in the population of head-group choline bonds in a trans-conformation, consistent with denser packing of the bilayer.

Influence of lipid phase on GLP-1 association with a supported bilayer. The DMPC phospholipid experiments presented above were carried out at 21°C, which falls in the middle of the broad (~8ºC) melting transition of the DMPC supported-bilayer.[17] To assess the impact of phospholipid phase (above or below their melting transition) and to explore the corresponding contributions of the bilayer acyl-chain ordering on GLP-1 interactions, concentration-dependent GLP-1 coverages were measured for DPPC and POPC supported bilayers. At 21°C, these bilayers were well below the 44°C melting transition of DPPC and well above the -2°C melting transition of POPC. Samples were prepared by mixing small aliquots of lipid-bilayer-modified particles (POPC or DPPC) with GLP-1 solutions and diluted with 50-mM phosphate buffer to produce samples with GLP-1 concentrations ranging from 0 to 50 µM. Raman spectra were acquired from five different particles for each sample. Following baseline correction, spectra from the five particles were normalized to the intensity of the phospholipid carbonyl stretch and averaged, and the results are provided in Supporting Information (Figure S3). The concentration-dependent lipid-bilayer associated GLP-1 populations from these spectra for DPPC and POPC bilayers were determined and plotted, along with their corresponding Langmuir isotherm fits in Figure 5, together with DMPC results

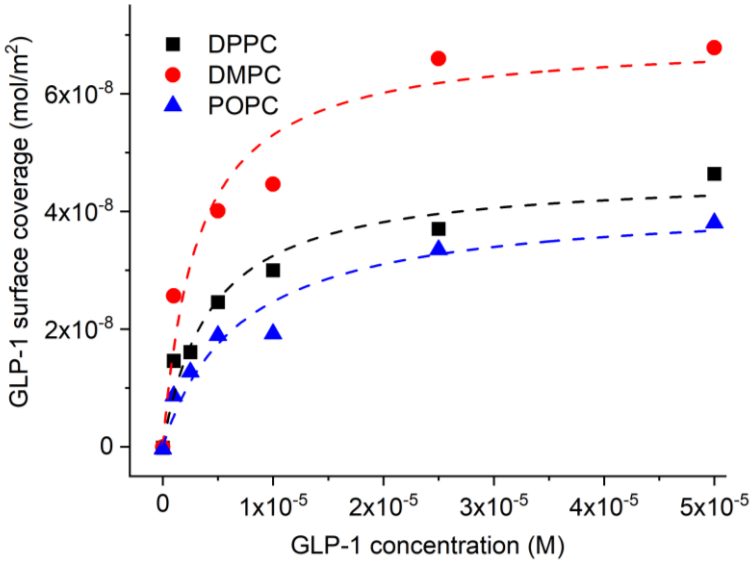

Figure 5. GLP surface coverages on POPC (blue triangles), DMPC (red circles), and DPPC (black squares) bilayers, with corresponding Langmuir isotherm fits (lines).

for comparison. Both the DPPC and POPC isotherms show comparable maximum GLP-1 coverages, Γ_{max}=4.3±0.4 x10^{-8} and 3.9±0.5 x10^{-8} mol/m^2, respectively, but these are both lower compared to Γ_{max}=6.4±0.4 x10^{-8} mol/m^2 for DMPC bilayers, determined above. This result shows that a lipid membrane at a temperature within its melting transition appears to accommodate a greater population of peptides at maximum coverage compared to either a gel-phase or fluid-phase membrane. This is perhaps not surprising given evidence of the insertion of GLP-1 within the DMPC bilayer above. It has been shown that phase-boundary defects exist in a bilayer within its melting transition due to differences in lipid density between regions of the bilayer in the gel and liquid crystalline phases.[53,55,56] These phase-boundaries could increase the capacity of the bilayer to accommodate peptide and lower the free energy cost to membrane insertion of the peptide, as considered in the following paragraph.

To explore the energetics of GLP-1-membrane affiliation, the fit of the measured isotherms to the Langmuir model can be used to determine the Langmuir constant for GLP-1 sorption into the supported bilayer. The Langmuir constants determined from a fit of the isotherms are K_L = 2.3±0.2 x10^5 M^{-1}, 3.2±0.2 x10^5 M^{-1}, and 1.4±0.2 x10^5 M^{-1} for DPPC, DMPC, and POPC, respectively. The results show that the peptide indeed partitions more favorably into a DMPC bilayer than into either a DPPC or POPC bilayer. As suggested above by the Γ_{max} results, the presence of phase-boundary defects in a lipid membrane near its phase transition appear to lower the free energy cost of accommodating a peptide in the DMPC bilayer, thereby increasing the observed Langmuir constant. The fluid-phase bilayer, POPC, was found to exhibit a weaker affinity for the peptide compared to the saturated lipid phases, DMPC or DPPC. This result is surprising in view of liquid-disordered lipid phases being generally better environments for small-molecule solutes.[57] In this case, however, an explanation may be found in the greater increase in acyl-chain order observed in the DMPC and DPPC bilayers when GLP-1 affiliates with saturated-lipid membrane (see Figure 6 below). The energy cost for the acyl chains of POPC to adopt an ordered structure in order to provide free-volume for GLP-1 affiliation should be greater, since its melting temperature is more than 20°C below the temperature at which the experiments were performed.

To examine the influence of GLP-1 on the structures of the gel-phase and fluid-phase bilayers, the fitted isotherms from Figure 5 were used in a linear-least-squares analysis, as above, to investigate the impact of peptide accumulation on the Raman spectra of DPPC and POPC bilayers. The fixed and Langmuir-isotherm spectral components from this analysis are presented in Figure 6, together with the component spectra of DMPC for comparison. In all three cases, Raman features from the bilayer-associated peptide (phenylalanine ring breathing mode, tryptophan Fermi doublet, backbone amide modes) appear in the Langmuir-isotherm component, as expected. Similar changes in intensity in phospholipid Raman bands are also observed. Most notably, there is a consistent and significant increase in carbon-carbon trans conformers, a decrease in carbon-carbon gauche conformer intensities, a sharpening of the CH_2 twist, and a correlation-field splitting of the CH_2 bending mode, all of which indicate ordering of the lipid acyl chains with GLP-1 accumulation. There is also a shifting of the symmetric CN head-group stretch indicating an increase in choline trans-character consistent with a decrease in the average spacing between lipid head-groups due to the local increase in lipid density. These results suggest that the GLP-1 association influences both head-group and acyl-chain regions of the lipid bilayer regardless of the initial lipid bilayer phase. The relative intensity changes in the head-group CN stretch are more significant in the case of the POPC bilayer, as compared to changes in its acyl chain trans-conformer carbon-carbon stretch. This may arise from the peptide preferentially associating with the head-group region of fluid-

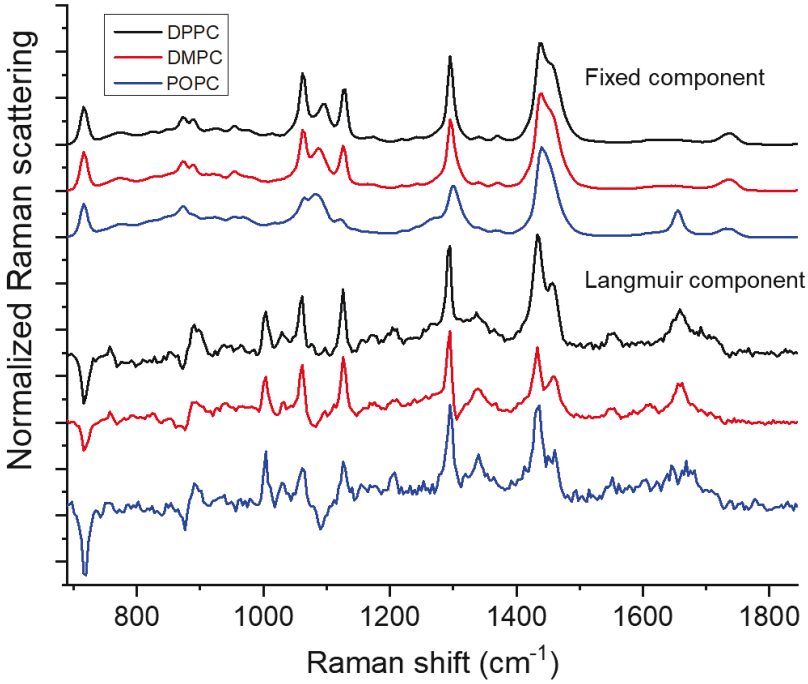

Figure 6. Component spectra from linear-least-squares analysis of Raman spectra from POPC (blue), DMPC (red), and DPPC (black) supported bilayer particles exposed to variable concentrations of GLP-1 in solution. Presented are the fixed component (top) and the concentration-dependent component defined by the Langmuir fit of the GLP-1 surface coverage (bottom). Band assignments are in Figure 4 and discussed in the text.

phase bilayers because of a greater energy cost of ordering the unsaturated acyl chains that are well above their melting temperature, thereby producing a smaller Langmuir constant and maximum surface coverage (see above).

Peptide-bilayer affiliation in the low-concentration limit: impact of dye labeling. The inverse of the Langmuir constant indicates the solution concentration at which a lipid bilayer is half-saturated with an adsorbate (see Equation 2). For the present system, these concentrations are in the 5- to 10-μM range, while natural and therapeutic concentrations of GLP-1 are 4 orders-of-magnitude lower, on the order of 10^{-10} M.[58] At such low concentrations, the binding of peptide is linear with concentration, where Equation 2 reduces to:

$$\Gamma = \Gamma_{max} K_L [GLP1] = K_{eq} [GLP1] * 1000 \qquad (5)$$

where K_{eq} is the equilibrium constant that predicts the surface concentration of GLP-1, Γ in mol/m^2, for a given solution concentration, [*GLP*1] in mol/liter, where the factor 1000 converts the solution concentration to mol/m^3. This equilibrium constant in the limit of low concentrations of peptide, $K_{eq} = \Gamma_{max} K_L$ /1000, is the ratio of the surface population in mol/m^2 to the solution concentration in mol/m^3 and has units of distance in meters. K_{eq} represents, for an arbitrary area of lipid bilayer, the distance into solution that the area must be projected to find the same number of solution-phase molecules as reside at equilibrium in the lipid bilayer.[12,59,60] This equilibrium constant characterizes the ratio of surface-to-solution concentrations in the linear region of the isotherm and is appropriate to use for characterizing membrane affinity of natural and therapeutic concentrations of peptide. The resulting equilibrium constants in this low-concentration limit determined from the isotherms in Figure 5 are: K_{eq} = 10±3 μm, 21±5 μm, and 6±2 μm for DPPC, DMPC, and POPC, respectively. These results show a stronger relative association of GLP-1 with the DMPC bilayer, 2-fold greater than DPPC and 3-fold greater than POPC; the trend in K_{eq} in this low-concentration region follows the same order as the Langmuir constants, but with a greater relative affinity observed for DMPC in the low-concentration regime arising from the larger Γ_{max} value for a bilayer at a temperature within its main phase transition.

The determination of K_{eq} in the low-concentration limit allows comparison of unlabeled GLP-1 in particle-supported lipid bilayers determined by Raman microscopy with single-

molecule-counting measurements of fluorescently-labeled GLP-1 populations on planar DPPC bilayers.[12] The fluorescent label in that study was separated from the peptide sequence by a 12-atom PEG spacer and utilized a charged dye label to increase its water solubility. The affinity of the dye and linker fragment for a DPPC bilayer was not detectable in control experiments, and there was no difference in the GLP-1 affinity for DPPC when the label was on the N- versus C-terminus of the peptide.[12] Nevertheless, there can still be a concern about the impact of a label on the solvation or folding of the peptide that would impact its membrane affiliation. The measured equilibrium constant for unlabeled GLP-1 accumulation in the within-particle supported DPPC bilayer, K_{eq} = 10±3 μm, is 2.8-times greater than the equilibrium constant measured by single-molecule-counting of labeled GLP-1 interacting with DPPC planar-supported bilayers, K_{eq} = 3.6±0.2 μm.[12] While the equilibrium constants are of similar magnitude, the smaller equilibrium constant for the labeled peptide result shows the significant influence of the dye label on GLP-1 membrane affinity. While some of this difference could be due to the influence of the curved support surface of the porous silica substrate, supported-lipid bilayers in wide-pore silica have been shown to have comparable structure, organization, and melting-transition behavior as planar-supported bilayers,[17] suggesting that surface-curvature effects should be small. The smaller lipid-bilayer association of the dye-labeled GLP-1 more likely arises from interactions between the tethered dye label and the peptide in free solution, where the dye could inhibit initial affiliation of the solution-phase peptide with the bilayer; alternatively, the water-soluble dye and linker may interfere with the peptide adopting a minimum-energy conformation in the lipid bilayer.

CONCLUSIONS

Confocal Raman microscopy of peptide association with supported phospholipid bilayers deposited on the pore walls of silica particles has been used for the label-free quantification of bilayer associated GLP-1, an incretin signaling peptide. Membrane-association isotherms were measured for GLP-1 accumulation in supported DPPC, DMPC, and POPC model membranes, allowing label-free determination of GLP-1 equilibrium constants; membrane affiliation was greatest for DMPC within its melting transition, where presence of boundaries between the gel and

fluid phase domains may provide regions where conversion of disordered acyl-chains to gel-phase is facile, with a low energy barrier to providing free-volume to accommodate the bound peptide. Raman spectra acquired for peptide accumulation in the bilayer versus solution-phase GLP-1 concentration can be resolved into a fixed spectrum of the supported bilayer and a spectrum that reports the membrane-associated peptide and corresponding changes in the lipid bilayer as the peptide accumulates. The changes in bilayer structure from the Raman scattering data reflected an increase in the order of the acyl-chains of the bilayer and trans-choline head-group populations as GLP-1 accumulates in the bilayer. This ordering of the acyl chains differs from previously reported behavior of phospholipid vesicle membranes upon accumulation of helical peptides, where disordering of the bilayer is observed. This difference is likely due to vesicle membranes being able to expand their area to accommodate the intercalated peptide, while supported lipid bilayers are constrained by the fixed-area of their supports. For supported bilayers, the local lipid density must apparently increase through chain-ordering to create the free volume needed a peptide to intercalate in the bilayer. This result raises questions about whether studies of membrane affinity of peptides on supported lipid bilayers can accurately predict their behavior in vesicle or cell membranes. Our lab plans to address this question by investigating the accumulation of GLP-1 into optically-trapped lipid vesicles[46] under the same conditions as the present study. Finally, the equilibrium constant for unlabeled GLP-1 affiliation with a DPPC bilayer in porous silica was compared with that of fluorescently-labeled GLP-1 binding to a planar-supported DPPC bilayer. A 3-fold larger equilibrium constant for the unlabeled peptide likely the influence of a dye label on GLP-1 membrane affinity, due either to dye-peptide interactions in free solution or to the dye inhibiting the peptide from adopting optimal conformations in the bilayer.

ASSOCIATED CONTENT

Supporting Information.

Additional information is provided on the reversibility of GLP-1 affiliation with DMPC bilayers, Raman scattering data from solution-phase standards for quantitative calibration, and Raman spectra of GLP accumulation in POPC and DPPC supported bilayers.

ACKNOWLEDGMENTS

This research was supported with funds from the National Science Foundation under Grants CHE-1608949 and CHE-1904424 and from the U.S. Department of Energy, Office of Basic Energy Sciences under Grant DE-FG03-93ER14333. Postdoctoral fellowship support for JPK from the Utah Center for Clinical and Translational Science, funded by the NIH-NLM Training Grant T15 LM00712418, is gratefully acknowledged.

REFERENCES

(1) Sargent, D.F.; Schwyzer, R. Membrane lipid phase as catalyst for peptide-receptor interactions. *Proc. Natl. Acad. Sci. U. S. A.* **1986**, *83*, 5774-5778.

(2) Castanho, M.A.R.B.; Fernandes, M.X. Lipid membrane-induced optimization for ligand-receptor docking: recent tools and insights for the "membrane catalysis" model. *Eur. Biophys. J.* **2006**, *35*, 92-103.

(3) Langelaan, D.N.; Rainey, J.K. Membrane catalysis of peptide-receptor binding. *Biochem. Cell Biol.* **2010**, *88*, 203-210.

(4) Holst, J.J. The Physiology of Glucagon-like Peptide 1. *Physiol. Rev.* **2007**, *87*, 1409-1439.

(5) Grieve, D.J.; Cassidy, R.S.; Green, B.D. Emerging cardiovascular actions of the incretin hormone glucagon-like peptide-1: potential therapeutic benefits beyond glycaemic control? *Br. J. Pharmacol.* **2009**, *157*, 1340-1351.

(6) Green, B.D.; Flatt, P.R. Incretin hormone mimetics and analogues in diabetes therapeutics. *Best Pract. Res., Clin. Endocrinol. Metab.* **2007**, *21*, 497-516.

(7) Yang, P.-Y.; Zou, H.; Chao, E.; Sherwood, L.; Nunez, V.; Keeney, M.; Ghartey-Tagoe, E.; Ding, Z.; Quirino, H.; Luo, X.; Welzel, G.; Chen, G.; Singh, P.; Woods, A.K.; Schultz, P.G.; Shen, W. Engineering a long-acting, potent GLP-1 analog for microstructure-based transdermal delivery. *Proc. Natl. Acad. Sci. U. S. A.* **2016**, *113*, 4140.

(8) Kim, Y.; Rose, C.A.; Liu, Y.; Ozaki, Y.; Datta, G.; Tu, A.T. FT-IR and Near-Infared FT-Raman Studies of the Secondary Structure of Insulinotropin in the Solid State: α-Helix to β-Sheet Conversion Induced by Phenol and/or by High Shear Force. *J. Pharm. Sci.* **1994**, *83*, 1175-1180.

(9) Thornton, K.; Gorenstein, D.G. Structure of Glucagon-Like Peptide(7-36) Amide in a Dodecylphosphocholine Micelle as Determined by 2D NMR. *Biochemistry* **1994**, *33*, 3532-3539.

(10) Neidigh, J.W.; Fesinmeyer, R.M.; Prickett, K.S.; Andersen, N.H. Exendin-4 and Glucagon-like-peptide-1: NMR Structural Comparisons in the Solution and Micelle-Associated States. *Biochemistry* **2001**, *40*, 13188-13200.

(11) Fox, C.B.; Wayment, J.R.; Myers, G.A.; Endicott, S.K.; Harris, J.M. Single-Molecule Fluorescence Imaging of Peptide Binding to Supported Lipid Bilayers. *Anal. Chem.* **2009**, *81*, 5130-5138.

(12) Myers, G.A.; Gacek, D.A.; Peterson, E.M.; Fox, C.B.; Harris, J.M. Microscopic Rates of Peptide–Phospholipid Bilayer Interactions from Single-Molecule Residence Times. *J. Am. Chem. Soc.* **2012**, *134*, 19652-19660.

(13) Thomas, G.J. Raman Spectroscopy of Protein and Nucleic Acid Assemblies. *Annu. Rev. Biophys. Biomol. Struct.* **1999**, *28*, 1-27.

(14) Tuma, R. Raman spectroscopy of proteins: from peptides to large assemblies. *J. Raman Spectrosc.* **2005**, *36*, 307-319.

(15) Gaber, B.P.; Peticolas, W.L. On the quantitative interpretation of biomembrane structure by Raman spectroscopy. *Biochim. Biophys. Acta, Biomembr.* **1977**, *465*, 260-274.

(16) Schultz, Z.D.; Levin, I.W. Vibrational spectroscopy of biomembranes. *Annu Rev Anal Chem (Palo Alto Calif)* **2011**, *4*, 343-366.

(17) Bryce, D.A.; Kitt, J.P.; Harris, J.M. Confocal-Raman Microscopy Characterization of Supported Phospholipid Bilayers Deposited on the Interior Surfaces of Chromatographic Silica. *J. Am. Chem. Soc.* **2018**, *140*, 4071–4078.

(18) Bryce, D.A.; Kitt, J.P.; Harris, J.M. Confocal Raman Microscopy for Label-Free Detection of Protein–Ligand Binding at Nanopore-Supported Phospholipid Bilayers. *Anal. Chem.* **2018**, *90*, 11509-11516.

(19) Kitt, J.P.; Harris, J.M. Confocal Raman Microscopy for in Situ Detection of Solid-Phase Extraction of Pyrene into Single C18–Silica Particles. *Anal. Chem.* **2014**, *86*, 1719-1725.

(20) Kitt, J.P.; Bryce, D.A.; Minteer, S.D.; Harris, J.M. Confocal Raman Microscopy for in Situ Measurement of Phospholipid–Water Partitioning into Model Phospholipid Bilayers within Individual Chromatographic Particles. *Anal. Chem.* **2018**, *90*, 7048-7055.

(21) Houlne, M.P.; Sjostrom, C.M.; Uibel, R.H.; Kleimeyer, J.A.; Harris, J.M. Confocal Raman Microscopy for Monitoring Chemical Reactions on Single Optically Trapped, Solid-Phase Support Particles. *Anal. Chem.* **2002**, *74*, 4311-4319.

(22) Bridges, T.E.; Houlne, M.P.; Harris, J.M. Spatially Resolved Analysis of Small Particles by Confocal Raman Microscopy: Depth Profiling and Optical Trapping. *Anal. Chem.* **2004**, *76*, 576-584.

(23) Williams, K.P.J.; Pitt, G.D.; Batchelder, D.N.; Kip, B.J. Confocal Raman Microspectroscopy Using a Stigmatic Spectrograph and CCD Detector. *Appl. Spectrosc.* **1994**, *48*, 232-235.

(24) Korzeniewski, C.; Kitt, J.P.; Bukola, S.; Creager, S.E.; Minteer, S.D.; Harris, J.M. Single Layer Graphene for Estimation of Axial Spatial Resolution in Confocal Raman Microscopy Depth Profiling. *Anal. Chem.* **2019**, *91*, 1049-1055.

(25) Haaland, D.M.; Easterling, R.G.; Vopicka, D.A. Multivariate Least-Squares Methods Applied to the Quantitative Spectral Analysis of Multicomponent Samples. *Appl. Spectrosc.* **1985**, *39*, 73-84.

(26) Beebe, K.R.; Kowalski, B.R. An Introduction to Multivariate Calibration and Analysis. *Anal. Chem.* **1987**, *59*, 1007A-1017A.

(27) Franke, J.E. In *Handbook of Vibrational Spectroscopy*; Chalmers, J.M., Griffiths, P.R., Eds.; John Wiley & Sons, Ltd: Chichester, 2002; Vol. 3.

(28) Kitt, J.P.; Harris, J.M. Confocal Raman Microscopy of Hybrid-Supported Phospholipid Bilayers within Individual C18-Functionalized Chromatographic Particles. *Langmuir* **2016**, *32*, 9033-9044.

(29) Rygula, A.; Majzner, K.; Marzec, K.M.; Kaczor, A.; Pilarczyk, M.; Baranska, M. Raman spectroscopy of proteins: a review. *J. Raman Spectrosc.* **2013**, *44*, 1061-1076.

(30) Kučerka, N.; Kiselev, M.A.; Balgavý, P. Determination of bilayer thickness and lipid surface area in unilamellar dimyristoylphosphatidylcholine vesicles from small-angle neutron scattering curves: a comparison of evaluation methods. *Eur. Biophys. J.* **2004**, *33*, 328-334.

(31) Sun, S.; Luo, N.; Ornstein, R.L.; Rein, R. Protein structure prediction based on statistical potential. *Biophys J* **1992**, *62*, 104-106.

(32) Zagrovic, B.; Jayachandran, G.; Millett, I.S.; Doniach, S.; Pande, V.S. How Large is an [alpha]-Helix? Studies of the Radii of Gyration of Helical Peptides by Small-angle X-ray Scattering and Molecular Dynamics. *J. Mol. Biol.* **2005**, *353*, 232-241.

(33) Rivera, D.; Harris, J.M. In Situ Studies of Pyridine Adsorption to Bare and Cyano-Derivatized Silica Sol−Gel Films Using Attenuated-Total-Internal-Reflection Fourier-Transform Infrared Spectroscopy. *Langmuir* **2001**, *17*, 5527-5536.

(34) Levin, I.W. Vibrational spectroscopy of membrane assemblies. *Adv Infrared Raman Spec* **1984**, *11*, 1-48.

(35) Levin, I.W.; Bush, S.F. Evidence for acyl chain trans/gauche isomerization during the thermal pretransition of dipalmitoyl phosphatidylcholine bilayer dispersions. *Biochim. Biophys. Acta, Biomembr.* **1981**, *640*, 760-766.

(36) Lippert, J.L.; Peticolas, W.L. Raman active vibrations in long-chain fatty acids and phospholipid sonicates. *Biochim. Biophys. Acta, Biomembr.* **1972**, *282*, 8-17.

(37) Orendorff, C.J.; Ducey, M.W.; Pemberton, J.E. Quantitative Correlation of Raman Spectral Indicators in Determining Conformational Order in Alkyl Chains. *J. Phys. Chem. A* **2002**, *106*, 6991-6998.

(38) Schultz, Z.D.; Levin, I.W. Lipid Microdomain Formation: Characterization by Infrared Spectroscopy and Ultrasonic Velocimetry. *Biophys. J.* **2008**, *94*, 3104-3114.

(39) Csiszár, A.; Koglin, E.; Meier, R.J.; Klumpp, E. The phase transition behavior of 1,2-dipalmitoyl-sn-glycero-3-phosphocholine (DPPC) model membrane influenced by 2,4-dichlorophenol—an FT-Raman Spectroscopy Study. *Chem. Phys. Lipids* **2006**, *139*, 115-124.

(40) Fox, C.B.; Uibel, R.H.; Harris, J.M. Detecting Phase Transitions in Phosphatidylcholine Vesicles by Raman Microscopy and Self-Modeling Curve Resolution. *J. Phys. Chem. B* **2007**, *111*, 11428-11436.

(41) Kitt, J.P.; Bryce, D.A.; Harris, J.M. Calorimetry-Derived Composition Vectors to Resolve Component Raman Spectra in Phospholipid Phase Transitions. *Appl. Spectrosc.* **2016**, 0003702816652359.

(42) Levin, I.W.; Lavialle, F.; Mollay, C. Comparative effects of melittin and its hydrophobic and hydrophilic fragments on bilayer organization by Raman spectroscopy. *Biophys. J.* **1982**, *37*, 339-349.

(43) Brauner, J.W.; Mendelsohn, R.; Prendergast, F.G. Attenuated total reflectance Fourier transform infrared studies of the interaction of melittin, two fragments of melittin, and .delta.-hemolysin with phosphatidylcholines. *Biochemistry* **1987**, *26*, 8151-8158.

(44) Williams, R.W.; Starman, R.; Taylor, K.M.P.; Gable, K.; Beeler, T.; Zasloff, M.; Covell, D. Raman spectroscopy of synthetic antimicrobial frog peptides magainin 2a and PGLa. *Biochemistry* **1990**, *29*, 4490-4496.

(45) Aranda, F.J.; Teruel, J.A.; Ortiz, A. Interaction of a synthetic peptide corresponding to the N terminus of canine distemper virus fusion protein with phospholipid vesicles: a biophysical study. *Biochimica et Biophysica Acta (BBA) - Biomembranes* **2003**, *1618*, 51-58.

(46) Fox, C.B.; Horton, R.A.; Harris, J.M. Detection of Drug−Membrane Interactions in Individual Phospholipid Vesicles by Confocal Raman Microscopy. *Anal. Chem.* **2006**, *78*, 4918-4924.

(47) Fox, C.B.; Harris, J.M. Confocal Raman microscopy for simultaneous monitoring of partitioning and disordering of tricyclic antidepressants in phospholipid vesicle membranes. *J. Raman Spectrosc.* **2010**, *41*, 498-507.

(48) Reeves, J.P.; Dowben, R.M. Water permeability of phospholipid vesicles. *The Journal of Membrane Biology* **1970**, *3*, 123-141.

(49) Cherney, D.P.; Bridges, T.E.; Harris, J.M. Optical Trapping of Unilamellar Phospholipid Vesicles: Investigation of the Effect of Optical Forces on the Lipid Membrane Shape by Confocal-Raman Microscopy. *Anal. Chem.* **2004**, *76*, 4920-4928.

(50) Cremer, P.S.; Boxer, S.G. Formation and Spreading of Lipid Bilayers on Planar Glass Supports. *The Journal of Physical Chemistry B* **1999**, *103*, 2554-2559.

(51) Pinazo, A.; Wen, X.; Liao, Y.-C.; Prosser, A.J.; Franses, E.I. Comparison of DLPC and DPPC in Controlling the Dynamic Adsorption and Surface Tension of Their Aqueous Dispersions. *Langmuir* **2002**, *18*, 8888-8896.

(52) Nagle, J.F. Lipid Bilayer Phase Transition: Density Measurements and Theory. *Proc. Natl. Acad. Sci. U. S. A.* **1973**, *70*, 3443.

(53) Xie, A.F.; Yamada, R.; Gewirth, A.A.; Granick, S. Materials Science of the Gel to Fluid Phase Transition in a Supported Phospholipid Bilayer. *Phys. Rev. Lett.* **2002**, *89*, 246103.

(54) Akutsu, H. Direct determination by Raman scattering of the conformation of the choline group in phospholipid bilayers. *Biochemistry* **1981**, *20*, 7359-7366.

(55) Blicher, A.; Wodzinska, K.; Fidorra, M.; Winterhalter, M.; Heimburg, T. The Temperature Dependence of Lipid Membrane Permeability, its Quantized Nature, and the Influence of Anesthetics. *Biophys. J.* **2009**, *96*, 4581-4591.

(56) WSzmodis, A.; Blanchette, C.; Longo, M.; Orme, C.; Parikh, A. Thermally induced phase separation in supported bilayers of glycosphingolipid and phospholipid mixtures. *Biointerphases* **2010**, *5*, 120-130.

(57) Baumgart, T.; Hunt, G.; Farkas, E.R.; Webb, W.W.; Feigenson, G.W. Fluorescence probe partitioning between Lo/Ld phases in lipid membranes. *Biochim. Biophys. Acta, Biomembr.* **2007**, *1768*, 2182-2194.

(58) Wettergren, A.; Schjoldager, B.; Mortensen, P.E.; Myhre, J.; Christiansen, J.; Holst, J.J. Truncated GLP-1 (proglucagon 78–107-amide) inhibits gastric and pancreatic functions in man. *Dig. Dis. Sci.* **1993**, *38*, 665-673.

(59) Hansen, R.L.; Harris, J.M. Measuring Reversible Adsorption Kinetics of Small Molecules at Solid/Liquid Interfaces by Total Internal Reflection Fluorescence Correlation Spectroscopy. *Anal. Chem.* **1998**, *70*, 4247-4256.

(60) Starr, T.E.; Thompson, N.L. Total Internal Reflection with Fluorescence Correlation Spectroscopy: Combined Surface Reaction and Solution Diffusion. *Biophys. J.* **2001**, *80*, 1575-1584.

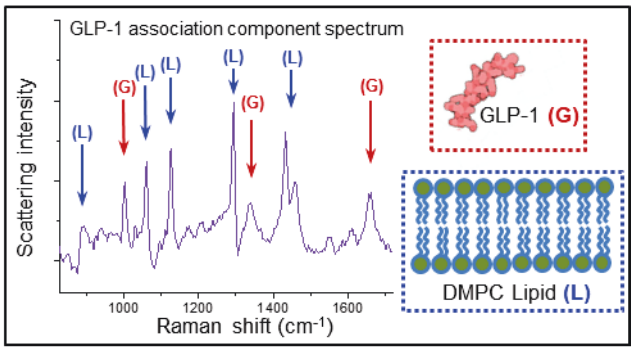

TOC Graphic